

Article

Microwave Dielectric Properties of CaB_2O_4 - CaSiO_3 System for LTCC Applications

Changzhi Yin ^{1,2}, Zhengyu Zou ³, Mingfei Cheng ^{1,2}, Yiyang Cai ^{1,2}, Jiaqing Yang ^{1,2}, Weicheng Lei ^{1,2},
Wenzhong Lu ^{1,2}, Xiaoqiang Song ^{1,2,*} and Wen Lei ^{1,2,*}

¹ Wenzhou Advanced Manufacturing Institute, Huazhong University of Science and Technology, Wenzhou 325035, China

² Key Laboratory of Functional Materials for Electronic Information (B) of MOE, School of Optical and Electronic Information, Huazhong University of Science and Technology, Wuhan 430074, China

³ Aerospace Nanhu Electronic Information Technology Co., Ltd., Wuhan 430074, China

* Correspondence: songxq@mail.hust.edu.cn (X.S.); wenlei@mail.hust.edu.cn (W.L.)

Abstract: A novel composite ceramic with low densification temperature was fabricated using the conventional solid-state method. The XRD and Rietveld refinement results indicated that the two phases of CaB_2O_4 and CaSiO_3 can coexist in all compositions. Furthermore, a phase transition of CaSiO_3 ceramic from α -phase to β -phase was observed. A dense ceramic with excellent microwave dielectric properties ($\epsilon_r \sim 6.4$, $Q \times f \sim 75,600$ GHz, and a negative $\tau_f \sim -26.9$ ppm/ $^\circ\text{C}$) was obtained at $x = 0.5$ when sintered at 925 $^\circ\text{C}$ at the frequency of 14.2 GHz. A good chemical compatibility between the composite ceramic and Ag electrode was improved by elemental mapping results. A patch antenna was fabricated based on the simulated result. All results indicated that the $0.5 \text{ CaB}_2\text{O}_4 + 0.5 \text{ CaSiO}_3$ ceramic has large application potential in the LTCC field.

Keywords: low permittivity; LTCC; dielectric properties; patch antenna



Citation: Yin, C.; Zou, Z.; Cheng, M.; Cai, Y.; Yang, J.; Lei, W.; Lu, W.; Song, X.; Lei, W. Microwave Dielectric Properties of CaB_2O_4 - CaSiO_3 System for LTCC Applications. *Crystals* **2023**, *13*, 790. <https://doi.org/10.3390/cryst13050790>

Academic Editor: Alexei A. Bokov

Received: 2 April 2023

Revised: 25 April 2023

Accepted: 4 May 2023

Published: 9 May 2023



Copyright: © 2023 by the authors. Licensee MDPI, Basel, Switzerland. This article is an open access article distributed under the terms and conditions of the Creative Commons Attribution (CC BY) license (<https://creativecommons.org/licenses/by/4.0/>).

1. Introduction

In recent years, the multilayer ceramic substrate has attracted much attention owing to its high capacity and low cost. The LTCC (low-temperature co-fired ceramics) technology has been widely used as a new method to achieve multilayer structures [1–4]. The LTCC technology can embed the passive components into a multilayer ceramic substrate with precious metals, such as Ag, Al, Cu, and interconnections [5–7].

Although the LTCC technology exhibits many advantages, there are also many preconditions that most ceramics cannot meet for use in the LTCC technology. For example, the substrate materials should have high strength, good insulation, and suitable thermal expansion coefficient [5]. Meanwhile, high relative density and good crystallization are obligatory for achieving good mechanical and dielectric properties. The low densification leads to low mechanical and poor dielectric properties. Scholars explored the glass composite by dividing it into high-softening-point glass and low-softening glass, which can meet the above requirements of the LTCC technology [8]. The composite ceramic has the superiority of avoiding the consequence caused by the interaction between refractory filler and glass, achieving high densification, optimizing the dielectric properties, and tailoring mechanical properties. As one of the attractive materials, calcium borosilicate glass ($\text{CaO-B}_2\text{O}_3\text{-SiO}_2$, CBS) has attracted much attention owing to its low dielectric and dielectric loss, and similar thermal expansion coefficient to the silicon chips [9–12]. In this system, the CaB_2O_4 and CaSiO_3 phase was easily crystallized at different B_2O_3 contents or the Ca/Si ratio [13]. For example, the CBS ceramic with a Ca/Si ratio of ~ 1.2 and a B_2O_3 content of 16.5% showed an excellent dielectric property ($\epsilon_r \sim 6.1$, $Q \times f \sim 11,700$ GHz) when sintered at 850 $^\circ\text{C}$ for 30 min [14]. As is well known, the sintering aids can significantly promote the densification procedure and decrease densification temperature. However, the unsuitable sintering-aid

dosage caused the liquid residue to deteriorate the dielectric properties at the microwave range. Hence, this work selected the major composition of the CBS glass of CaB_2O_4 and CaSiO_3 to design the composition with $(1 - x)\text{CaB}_2\text{O}_4 + x\text{CaSiO}_3$ ($x = 0, 0.2, 0.4, 0.5, 0.6, 0.8, \text{ and } 1$). The objective is to analyze the phase composition, sintering characteristics, microstructure, microwave dielectric properties, and mechanical behavior.

2. Experimental Procedure

The CaCO_3 , H_3BO_3 , and SiO_2 were weighed according to the chemical formulas CaB_2O_4 and CaSiO_3 , respectively. All materials had a high purity, above 99.8%. The powders were ball-milled for 12 h with alcohol and deionized water as the medium, respectively. The slurries were dried at 70 °C for 12 h and then calcinated at 700 °C for 3 h (CaB_2O_4) and 1175 °C for 12 h (CaSiO_3), respectively. The resulting powders were weighted based on the ratio of $(1 - x)\text{CaB}_2\text{O}_4 + x\text{CaSiO}_3$ ($0 \leq x \leq 1$) and then remilled in the same condition as mentioned above. After drying, the powders were mixed with 5 wt.% PVA as the binder and pressed into a cylinder of $\Phi 12 \times 6$ mm. The green samples were firstly sintered at 550 °C for 2 h and then sintered at 900~1350 °C for 5 h.

X-ray diffraction with $\text{CuK}\alpha$ radiation (XRD, XRD-7000, Shimadzu, Kyoto, Japan) was employed to analyze the phase composition. The crystal structure was determined using Rietveld refinement with GSAS and EXPGUI software. The thermal etching surfaces were observed using a scanning electron microscope (SEM, Sirion 200, Eindhoven, The Netherlands). The thermal etching temperatures were carried out at 50 °C lower than the optimum temperature. The flexural strength was measured using a universal testing machine (CMT1104NB). The dielectric properties of the ceramics were measured at microwave frequencies in the TE_{011} mode with the Hakki and Coleman method by using a vector network analyzer (Agilent E8362B, Agilent Technologies, St. Clara, CA, USA) [15]. Equation (1) was used to calculate τ_f over the temperature range of 25 °C to 80 °C:

$$\tau_f = \frac{1}{f(T_0)} \frac{[f(T_1) - f(T_0)]}{T_1 - T_0} \quad (1)$$

where $f(T_1)$ and $f(T_0)$ represent the resonant frequencies at T_1 (80 °C) and T_0 (25 °C), respectively. The CST Microwave Studio software was employed to simulate the geometrical parameter of a patch antenna.

3. Results and Discussion

Figure S1 (see supplementary materials) exhibits the X-ray patterns of the CaB_2O_4 and CaSiO_3 ceramics calcined at 700 °C and 1175 °C, respectively. The CaB_2O_4 peaks accompanied by a small amount of unknown phase can be detected and matched well with PDF # 075-0640, whereas the α - CaSiO_3 phase (PDF # 089-6585) coexists with a small amount of the SiO_2 phase. Figure 1 exhibits the X-ray patterns of $(1 - x)\text{CaB}_2\text{O}_4 + x\text{CaSiO}_3$ ($0 \leq x \leq 1$) sintered at their optimum temperature.

For the $x = 0$ composition, the second phase disappeared, indicating that the unknown phase was an interphase, and a pure CaB_2O_4 phase was obtained at 950 °C. When $0.2 \leq x \leq 0.8$, the coexistence of CaB_2O_4 and CaSiO_3 was detected with an interesting phenomenon; that is, the α - CaSiO_3 phase was transformed to the β - CaSiO_3 phase with the CaB_2O_4 doped. Meanwhile, the SiO_2 phase was not determined for all compositions. No phase transition was detected when the α - CaSiO_3 was sintered at 1350 °C for 3 h, indicating that the CaB_2O_4 ceramic can promote the CaSiO_3 phase transformation from α to β phase. Figure S2 shows the Rietveld refinement results to further conform the phase composition of $(1 - x)\text{CaB}_2\text{O}_4 + x\text{CaSiO}_3$. The red circle shows the measured data, whereas the black line represents the calculated data. The good agreement between them indicated that the results were reliable. All results indicated that only the CaB_2O_4 and CaSiO_3 phase existed, which further confirms the deficiency of chemical reaction between them. This case is an important factor in achieving component controllability.

Microstructure analysis gives further evidence for the chemical compatibility of the CaB_2O_4 and CaSiO_3 phases. Figure 2 exhibits the thermal etching microstructure and elemental mapping analysis of $0.5 \text{ CaB}_2\text{O}_4 + 0.5 \text{ CaSiO}_3$ ceramics sintered at their optimum temperature. A dense microstructure with two shapes of grain was observed. The elemental mapping analysis result indicated that the large grains can be indexed to the CaSiO_3 phase, whereas the small ones are identified as the CaB_2O_4 phase.

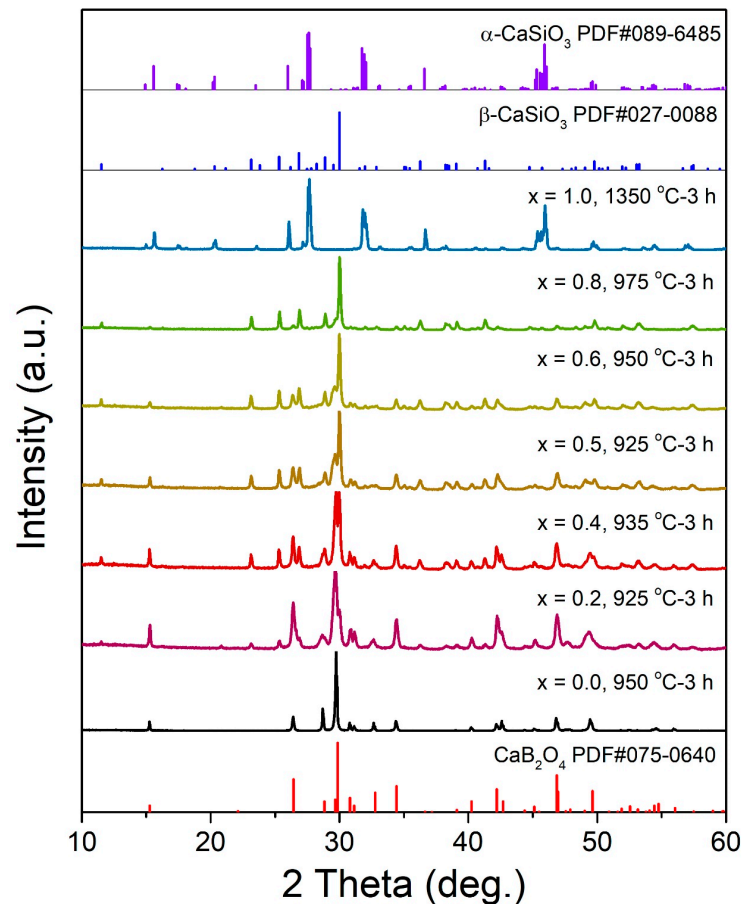


Figure 1. The X-ray data of $(1 - x)\text{CaB}_2\text{O}_4 + x\text{CaSiO}_3$ ($0 \leq x \leq 1$) sintered at their optimum temperature.

Figure 3 shows the density and flexural strength of $(1 - x)\text{CaB}_2\text{O}_4 + x\text{CaSiO}_3$ ceramics as a function of the x value. The bulk density shows a rising trend that increased from 2.6 g/cm^3 at $x = 0$ (with a relative density of $\sim 94.8\%$) to a maximum value of 2.7 g/cm^3 at $x = 0.5$ (with a relative density of $\sim 97.3\%$), then it decreased evidently as the content of CaSiO_3 further increased. As is well known, although the intrinsic characteristic of the material determines the theoretical flexural strength, the flexural strength is also proportional to the relative density. In other words, a high relative density means a high flexural strength, whereas a low relative density can result in a low flexural strength. As shown in Figure 3, the CaB_2O_4 ceramic has a low flexural strength, which can be attributed to the low relative density. By contrast, a high flexural strength with 170 MPa was obtained at the $x = 0.5$ composition, but the flexural strength decreased as the content of CaSiO_3 further increased. These results indicate that the suitable addition of CaSiO_3 can significantly enhance the flexural strength of the composite ceramic.

Figure 4 shows the variation of microwave dielectric properties of $(1 - x)\text{CaB}_2\text{O}_4 + x\text{CaSiO}_3$ ceramics with different content of CaSiO_3 . With CaSiO_3 doping, the τ_f values were decreased, from $-21.1 \text{ ppm/}^\circ\text{C}$ to $-34.3 \text{ ppm/}^\circ\text{C}$. Generally, τ_f is sensitive to the phase transition and phase composition [16–19]. The linear decrease of τ_f can be attributed to the lower value of CaSiO_3 ($\tau_f \sim -34.3 \text{ ppm/}^\circ\text{C}$) ceramic compared with the CaB_2O_4

ceramic ($\tau_f \sim -21.1$ ppm/ $^{\circ}\text{C}$). The $Q \times f$ significantly increased from 23,600 GHz at $x = 0$ to 75,600 GHz at $x = 0.5$ ($\tan\delta = 1.64 \times 10^{-4}$) and then decreased evidently with further doping of CaSiO_3 , which shows a similar variation trend to the relative density. This result indicates that density is crucial in this system.

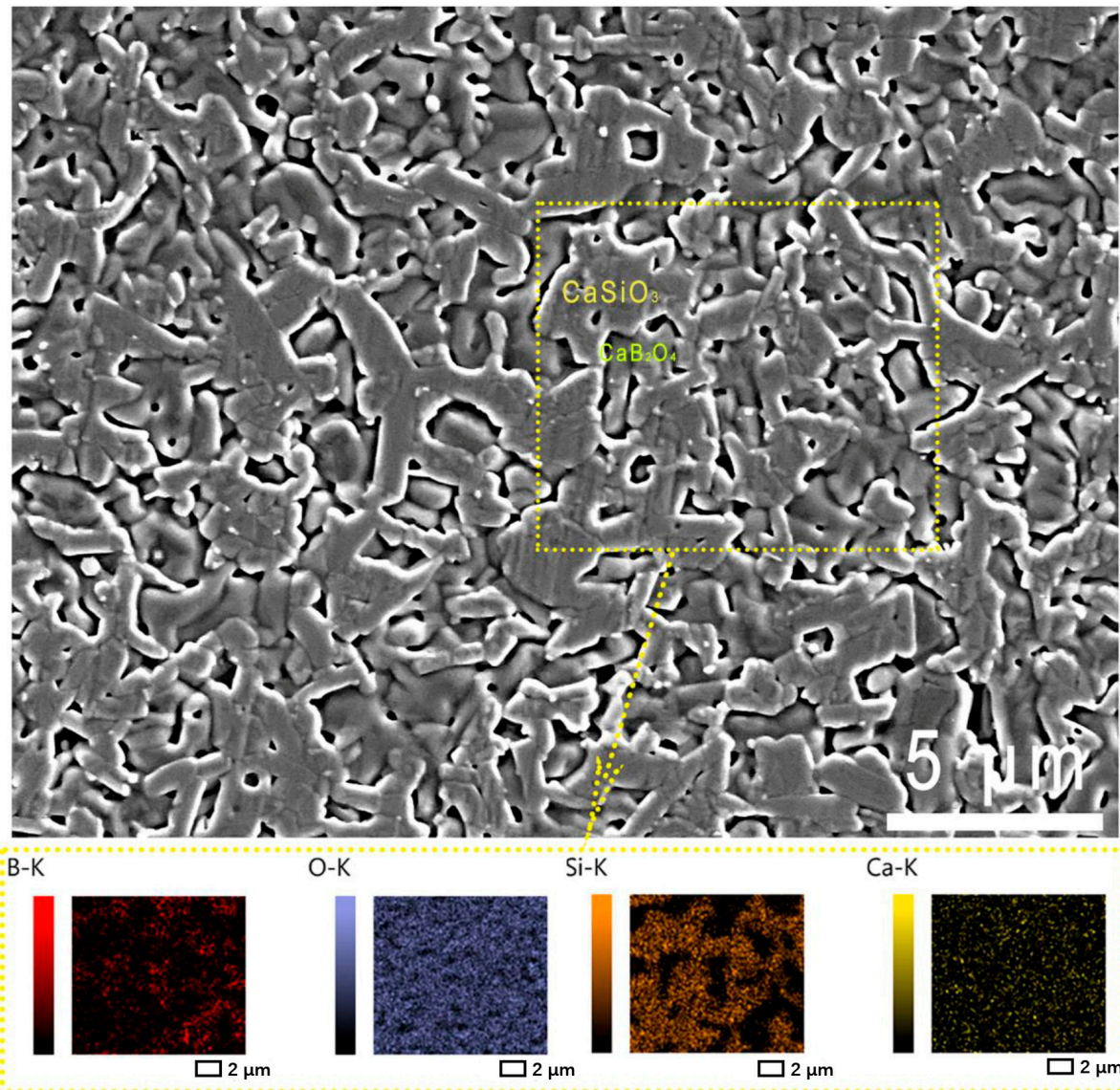


Figure 2. The microstructure and elemental mapping analysis result of $0.5\text{CaB}_2\text{O}_4 + 0.5\text{CaSiO}_3$ ceramics sintered at their optimum temperature.

The dielectric permittivity showed a slight growth trend from $x = 0$ to 0.8 and sharply increased at the $x = 1$ composition. This case can be attributed to the relatively low permittivity and high volume fraction of the CaB_2O_4 ceramic in this composite ceramic system. The Bosman and Having's equation can be employed to estimate the effect of porosity on the permittivity [20–22]:

$$\varepsilon_{\text{corr}} = \varepsilon_r(1 + 1.5P) \quad (2)$$

As shown in Figure 4, the measured values were lower than the measured ones and matched a minimum deviation at the $x = 0.5$ composition. A dense composite ceramic with comprehensive microwave dielectric properties was obtained at the $x = 0.5$ composition sintered at 925 $^{\circ}\text{C}$.

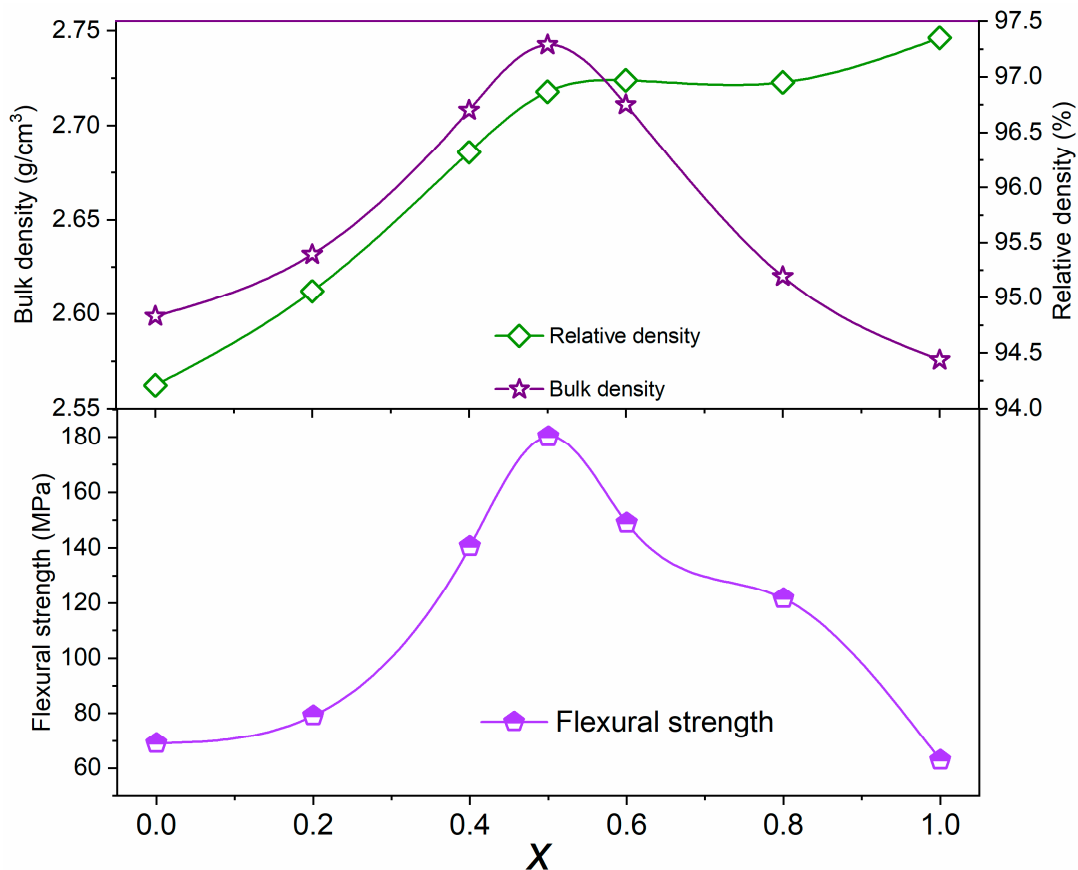


Figure 3. The density and flexural strength of $(1 - x)\text{CaB}_2\text{O}_4 + x\text{CaSiO}_3$ as a function of x value.

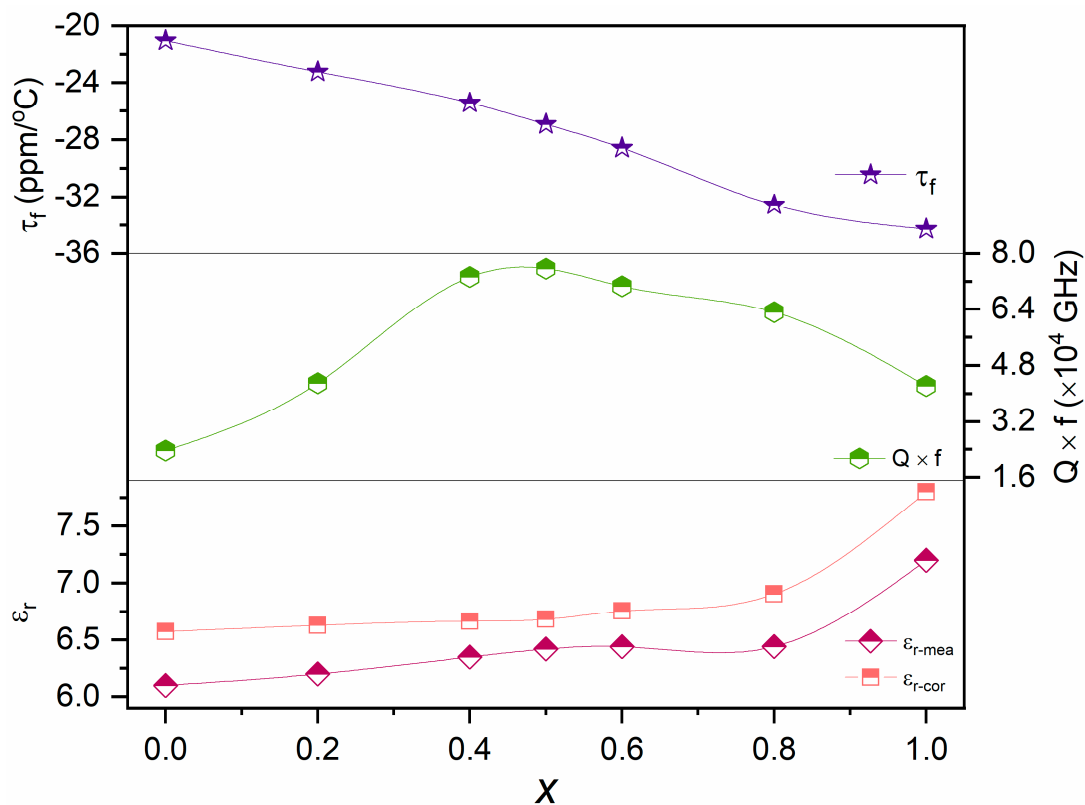


Figure 4. The microwave dielectric properties of $(1 - x)\text{CaB}_2\text{O}_4 + x\text{CaSiO}_3$ ceramics as a function of x value.

In recent years, the LTCC technology has attracted much attention owing to its advantages of high-frequency characteristics, high assembly density, thermal stability, and multifunctionality. The primary condition of the LTCC technology is the densification temperature of the ceramic lower than the melting point of the electrode, such as Ag at $\sim 961^\circ\text{C}$ and Cu at $\sim 1060^\circ\text{C}$. In this work, the $0.5\text{CaB}_2\text{O}_4 + 0.5\text{CaSiO}_3$ ceramics can be densified at 925°C , which meets the requirement of the LTCC technology. Figure 5 shows the elemental mapping results collected on the fracture surface of the $0.5\text{CaB}_2\text{O}_4 + 0.5\text{CaSiO}_3$ ceramic co-fired with the Ag electrode to estimate the application potential of this composite ceramic in the LTCC field. The clear boundary and distinct distribution of different elements indicate that the composite ceramic had good chemical compatibility with the Ag electrode.

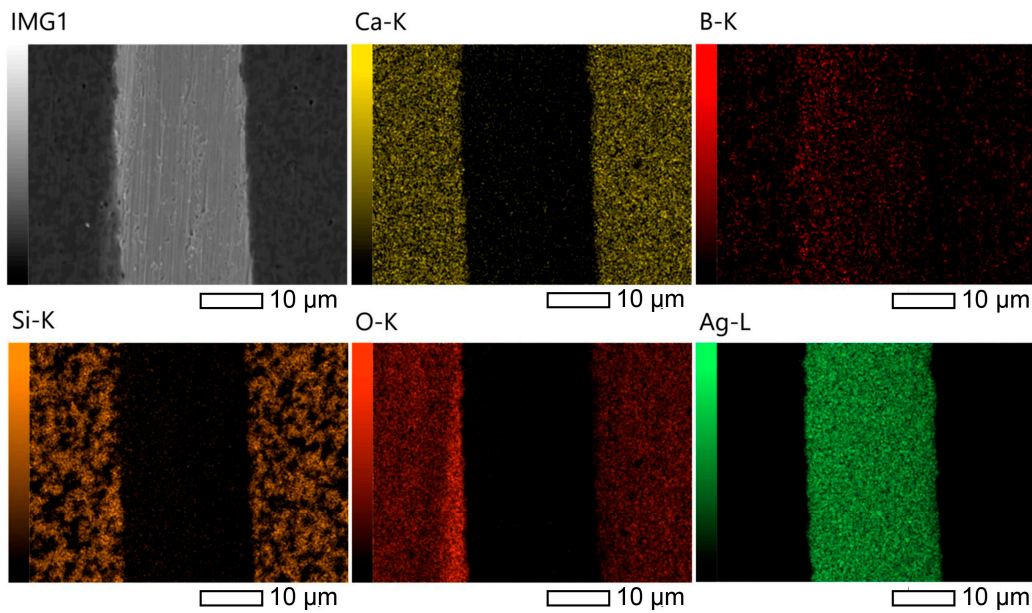


Figure 5. The fractured surface of $0.5\text{CaB}_2\text{O}_4 + 0.5\text{CaSiO}_3 + 20\text{ wt.}\% \text{Ag}$ sintered at 925°C and the elemental mapping analysis result.

A patch antenna was handmade using the $0.5\text{CaB}_2\text{O}_4 + 0.5\text{CaSiO}_3$ composite ceramic to confirm the application potential. Initially, the optimal configuration was simulated using the CST Microwave Studio software. Figure 6a shows the simulated geometry parameters of the patch antenna. Figure 6b presents the simulated and measured results of the S_{11} parameter. The center frequency of the simulated result was located at 6.6 GHz (impedance bandwidth of 80 MHz), whereas that of the measured result was localized at 6.62 GHz with a higher bandwidth of 94 MHz. Figure 6c,d show the radiation. The E and H planes showed nearly similar orientation radiation patterns. These results indicated that the $0.5\text{CaB}_2\text{O}_4 + 0.5\text{CaSiO}_3$ ceramic has potential applications in wireless communication systems.

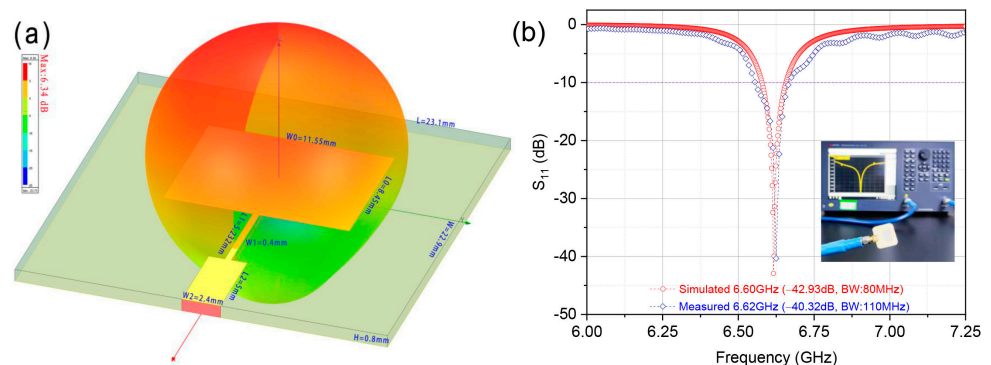


Figure 6. Cont.

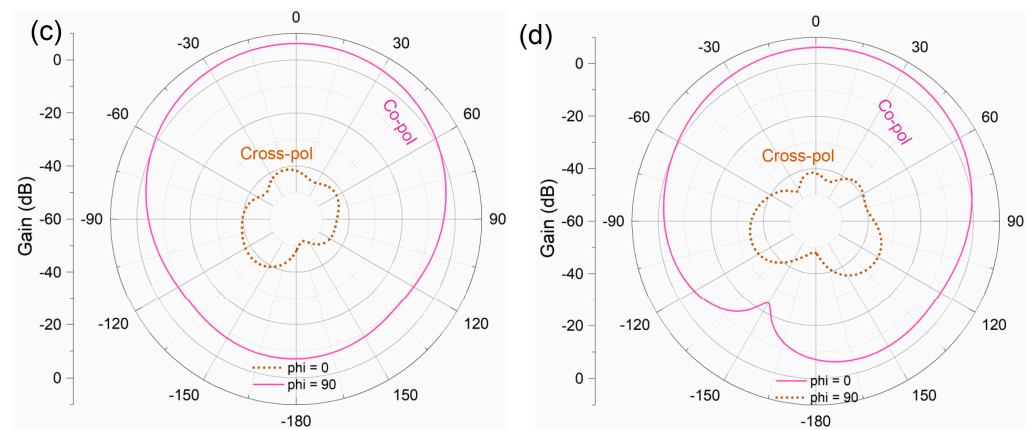


Figure 6. (a) The simulated geometry parameters of the patch antenna; (b) simulated and experimental S_{11} of the proposed antenna; (c) simulated radiation patterns of E and (d) H planes.

4. Conclusions

In this work, $(1 - x)\text{CaB}_2\text{O}_4 + x\text{CaSiO}_3$ composite ceramics with low densification temperature were prepared. The XRD and Rietveld refinement results indicate that the CaB_2O_4 and CaSiO_3 can coexist in all compositions. Furthermore, the CaB_2O_4 can promote the CaSiO_3 transformation from α -phase to β -phase. A dense ceramic with excellent microwave dielectric properties ($\epsilon_r \sim 6.4$, $Q \times f \sim 75,600$ GHz, and a negative $\tau_f \sim 26.9$ ppm/ $^\circ\text{C}$) was obtained at $x = 0.5$ when sintered at 925 $^\circ\text{C}$. The SEM image and elemental mapping results indicate that the $0.5\text{CaB}_2\text{O}_4 + 0.5\text{CaSiO}_3$ ceramic has good chemical compatibility with the Ag electrode. A patch antenna with a center frequency of 6 GHz and a high bandwidth was fabricated using the $0.5\text{CaB}_2\text{O}_4 + 0.5\text{CaSiO}_3$ ceramic. All results indicate that the $0.5\text{CaB}_2\text{O}_4 + 0.5\text{CaSiO}_3$ ceramic has large application potential in the LTCC field.

Supplementary Materials: The following supporting information can be downloaded at: <https://www.mdpi.com/article/10.3390/cryst13050790/s1>, Figure S1: The XRD patterns of calcined at different temperature of CaB_2O_4 and CaSiO_3 ; Figure S2: The Rietveld refinement results of $(1 - x)\text{CaB}_2\text{O}_4 + x\text{CaSiO}_3$; Figure S3: The microstructure of $(1 - x)\text{CaB}_2\text{O}_4 + x\text{CaSiO}_3$ ceramics sintered at their optimum temperature: (a) $x = 0.1$, (b) $x = 0.2$, (c) $x = 0.4$, (d) $x = 0.5$, (e) $x = 0.6$, (f) $x = 0.8$, (g) $x = 1$.

Author Contributions: Conceptualization, C.Y. and W.L. (Wen Lei); methodology, Z.Z.; software, M.C.; validation, Y.C. and J.Y.; formal analysis, C.Y.; investigation, Y.C. and W.L. (Weicheng Lei); resources, C.Y.; data curation, C.Y.; writing—original draft preparation, C.Y.; writing—review and editing, C.Y. and Z.Z.; visualization, X.S.; supervision, X.S. and W.L. (Wenzhong Lu); project administration, X.S. and W.L. (Wen Lei); funding acquisition, X.S. All authors have read and agreed to the published version of the manuscript.

Funding: This work was supported by the China Postdoctoral Science Foundation (2022M711233), National Natural Science Foundation of China (NSFC-U21B2068, 52072133, and 62061011), and the Basic Science and Technology Research Project of Wenzhou, Zhejiang Province (G20210019).

Institutional Review Board Statement: Not applicable.

Informed Consent Statement: Not applicable.

Data Availability Statement: Data is unavailable due to privacy.

Acknowledgments: This work was supported by the China Postdoctoral Science Foundation (2022M711233), National Natural Science Foundation of China (NSFC-U21B2068, 52072133, and 62061011), and the Basic Science and Technology Research Project of Wenzhou, Zhejiang Province (G20210019).

Conflicts of Interest: The authors declare no conflict of interest.

References

1. Sebastian, M.T. *Dielectric Materials for Wireless Communication*; Elsevier Publishers: Oxford, UK, 2008.
2. Sebastian, M.T.; Jantunen, H. Low loss dielectric materials for LTCC applications: A review. *Int. Mater. Rev.* **2008**, *53*, 57–90. [[CrossRef](#)]
3. Imanaka, Y. *Multilayered Low Temperature Cofired Ceramics (LTCC) Technology*; Springer Science & Business Media: Berlin/Heidelberg, Germany, 2005.
4. Zhou, D.; Randall, C.A.; Pang, L.X.; Wang, H.; Guo, J.; Zhang, G.Q.; Wu, Y.; Guo, K.T.; Shui, L.; Yao, X. Microwave dielectric properties of $(\text{ABi})_{1/2}\text{MoO}_4$ (A = Li, Na, K, Rb, Ag) type ceramics with ultra-low firing temperatures. *Mater. Chem. Phys.* **2011**, *129*, 688–692. [[CrossRef](#)]
5. Zhao, B.; Chen, X.; Chen, N.; Xu, X.; Lu, Y.; Cheng, J.; Wang, H. Low-temperature-sintered MgO-based microwave dielectric ceramics with ultralow loss and high thermal conductivity. *J. Am. Ceram. Soc.* **2023**, *106*, 1159–1169. [[CrossRef](#)]
6. Zhou, D.; Li, W.B.; Xi, H.H.; Pang, L.X.; Pang, G.S. Phase composition, crystal structure, infrared reflectivity and microwave dielectric properties of temperature stable composite ceramics (scheelite and zircon-type) in $\text{BiVO}_4\text{--YVO}_4$ system. *J. Mater. Chem. C* **2015**, *3*, 2582–2588. [[CrossRef](#)]
7. Li, C.C.; Yin, C.Z.; Khaliq, J.; Liu, L.J. Ultralow-temperature synthesis and densification of $\text{Ag}_2\text{CaV}_4\text{O}_{12}$ with improved microwave dielectric performances. *ACS Sustain. Chem. Eng.* **2021**, *9*, 14461–14469. [[CrossRef](#)]
8. Wang, S.F.; Wang, Y.R.; Hsu, Y.F.; Chiang, C.C. Densification and microwave dielectric behaviors of $\text{CaO--B}_2\text{O}_3\text{--SiO}_2$ glass-ceramics prepared from a binary glass composite. *J. Alloys Compd.* **2010**, *498*, 211–216. [[CrossRef](#)]
9. Chiang, C.C.; Wang, S.F.; Wang, Y.R.; Wei, W.C.J. Densification and microwave dielectric properties of $\text{CaO--B}_2\text{O}_3\text{--SiO}_2$ system glass-ceramics. *Ceram. Int.* **2008**, *34*, 599–604. [[CrossRef](#)]
10. Chang, C.R.; Jean, J.H. Crystallization kinetics and mechanism of low-dielectric, low-temperature, cofirable $\text{CaO--B}_2\text{O}_3\text{--SiO}_2$ glass-ceramics. *Int. J. Mater. Res.* **1999**, *82*, 1725–1732.
11. Wang, S.H.; Zhou, H.P. Densification and dielectric properties of $\text{CaO--B}_2\text{O}_3\text{--SiO}_2$ system glass ceramics. *Mater. Sci. Eng. B* **2003**, *99*, 597–600. [[CrossRef](#)]
12. Jean, J.H.; Chang, C.R.; Lei, C.D. Sintering of a crystallizable $\text{CaO--B}_2\text{O}_3\text{--SiO}_2$ glass with silver. *J. Am. Ceram. Soc.* **2004**, *87*, 1244–1249. [[CrossRef](#)]
13. Yamaguchi, S.; Takeuchi, T.; Ito, M.; Kokubo, T. $\text{CaO--B}_2\text{O}_3\text{--SiO}_2$ glass fibers for wound healing. *J. Mater. Sci. Mater. Med.* **2022**, *33*, 15. [[CrossRef](#)] [[PubMed](#)]
14. Yan, T.N.; Zhang, W.J.; Mao, H.J.; Chen, X.Y.; Bai, S.X. The effect of CaO/SiO_2 and B_2O_3 on the sintering contraction behaviors of $\text{CaO--B}_2\text{O}_3\text{--SiO}_2$ glass-ceramics. *Int. J. Mod. Phys. B* **2019**, *33*, 1950070. [[CrossRef](#)]
15. Hakki, B.W.; Coleman, P.D. A dielectric resonator method of measuring inductive capacities in the millimeter range. *IRE Trans. Microwave Theory Tech.* **1960**, *8*, 402–410. [[CrossRef](#)]
16. Yin, C.Z.; Du, K.; Zhang, M.; Yang, J.Q.; Wang, F.; Guo, Y.B.; Cheng, M.F.; Cai, Y.Y.; Song, X.Q.; Khaliq, J.; et al. Novel low- ϵ_r and lightweight LiBO_2 microwave dielectric ceramics with good chemical compatibility with silver. *J. Eur. Ceram. Soc.* **2022**, *42*, 4580–4586. [[CrossRef](#)]
17. Guo, H.X.; Zhu, P.S.; Lin, Q.P.; Gao, M.; Tang, D.P.; Zheng, X.H. Sintering characteristics and microwave dielectric properties of BaTi_4O_9 ceramics with CuO--TiO_2 addition. *Crystals* **2023**, *13*, 566. [[CrossRef](#)]
18. Du, K.; Song, X.Q.; Zou, Z.Y.; Fan, J.; Lu, W.Z.; Lei, W. Improved microwave dielectric properties of novel low-permittivity Sn-doped $\text{Ca}_2\text{HfSi}_4\text{O}_{12}$ ceramics. *Mater. Res. Bull.* **2020**, *129*, 110887. [[CrossRef](#)]
19. Zhou, X.; Liu, L.; Sun, J.; Zhang, N.; Sun, H.; Wu, H.; Tao, W. Effects of $(\text{Mg}_{1/3}\text{Sb}_{2/3})^{4+}$ substitution on the structure and microwave dielectric properties of $\text{Ce}_2\text{Zr}_3(\text{MoO}_4)_9$ ceramics. *J. Adv. Ceram.* **2021**, *10*, 778–789. [[CrossRef](#)]
20. Yoon, S.H.; Kim, D.; Cho, S.; Hong, K.S. Investigation of the relations between structure and microwave dielectric properties of divalent metal tungstate compounds. *J. Eur. Ceram. Soc.* **2006**, *26*, 2051–2054. [[CrossRef](#)]
21. Pan, H.L.; Cheng, L.; Wu, H.T. Relationships between crystal structure and microwave dielectric properties of $\text{Li}_2(\text{Mg}_{1-x}\text{Co}_x)_3\text{TiO}_6$ ($0 \leq x \leq 0.4$) ceramics. *Ceram. Int.* **2017**, *43*, 15018–15026. [[CrossRef](#)]
22. Xiong, Y.; Xing, Z.; Weng, J.H.; Ma, C.; Khaliq, J.; Li, C.C. Low-temperature sintering, dielectric performance, and far-IR reflectivity spectrum of a lightweight NaCaVO_4 with good chemical compatibility with silver. *Ceram. Int.* **2021**, *47*, 22219–22224. [[CrossRef](#)]

Disclaimer/Publisher's Note: The statements, opinions and data contained in all publications are solely those of the individual author(s) and contributor(s) and not of MDPI and/or the editor(s). MDPI and/or the editor(s) disclaim responsibility for any injury to person or property resulting from any ideas, methods, instructions or products referred to in the content.